



INQUA Focus Group Terrestrial Processes Perturbed by Tectonics
(TPPT)



paleoseismicity.org

Paleoseismic study of the XEOLXELEK–Elk Lake fault: A newly identified Holocene fault in the northern Cascadia forearc near Victoria, British Columbia, Canada

Harrichhausen, Nicolas (1)*, Theron Finley (2), Kristin D Morell (1), Christine Regalla (3), Scott E K Bennet (4), Lucinda J Leonard (2), Edwin Nissen (2), Eleanor McLeod (2), Emerson M Lynch (3), Guy Salomon (2), Israporn Sethanant (2)

(1) Department of Earth Science, University of California, Santa Barbara, CA, USA.

(2) School of Earth and Ocean Sciences, University of Victoria, Victoria BC, Canada

(3) School of Earth and Sustainability, Northern Arizona University, Flagstaff AZ, USA

(4) U.S. Geological Survey, Geology, Minerals, Energy, and Geophysics Science Center, Portland OR, USA

* Now at: Univ. Grenoble Alpes, Univ. Savoie Mont Blanc, CNRS, IRD, Univ. Gustave Eiffel, ISTerre, 38000 Grenoble, France.

Email: n.harrichhausen@univ-grenoble-alpes.fr

Abstract: High-resolution topographic data show a tectonic scarp formed in Quaternary sediments near the city of Victoria in the northern Cascadia forearc on Vancouver Island, British Columbia, Canada. A paleoseismic trench excavation across the structure, the XEOLXELEK–Elk Lake fault, shows evidence for a Holocene (after 12.2 cal ka BP) surface-rupturing reverse-slip earthquake that produced a fault-propagation fold and resulted in the formation of a ~1.4 to 3.5 m-high scarp. Fault-propagation fold modelling indicates ~3.2 m of reverse slip on a 50°-dipping fault plane reproduces the observed deformation, and fault-scaling relations suggest a single earthquake rupture with this surface displacement could occur during a ~ M_w 6.1–7.6 earthquake. Given the fault's location within the metropolitan area of Victoria, an earthquake near this magnitude would result in significant damage to local infrastructure and this fault is worth considering in future seismic hazard assessments.

Key words: Paleoseismic trench, Holocene rupture, Fault-propagation fold, Vancouver Island, Cascadia.

INTRODUCTION

Recent studies of Holocene surface-rupturing faults in the northern Cascadia forearc on Vancouver Island have highlighted the hazard they pose to this region. For instance, recognition of the Leech River fault as active and capable of producing ~M7 earthquakes (Fig. 1a, Morell et al., 2018) has resulted in modifications of seismic hazard assessments for Victoria, the capital city of British Columbia, Canada, with a metropolitan population of ~400,000 people (e.g., Kukovica et al., 2019). These new assessments show that the greatest increase in hazard occurs closest to the fault trace, highlighting the importance of accurately mapping active structures.

Northeast of Victoria, a bathymetric and seismic reflection study in the Haro Strait indicates potentially Quaternary-active, northwest-striking faults that connect with the Devils Mountain fault in Washington State, USA (Fig. 1a, Greene & Barrie, 2022). The northwest continuation of these structures project onshore across the Saanich Peninsula, within the metropolitan area of Victoria. We identified scarps formed in Quaternary sediments and bedrock scarps that cut across Saanich Peninsula and underneath XEOLXELEK (pronounced: hul-lakl-lik; also known as Elk Lake), along strike from the offshore structures (Fig. 1b). To assess whether this structure, the XEOLXELEK–Elk Lake fault (XELF), hosted recent surface-rupturing earthquakes, we excavated a paleoseismic trench across the Quaternary scarp in August, 2021 to examine the stratigraphy and deformation.

TOPOGRAPHIC ANALYSES

Analyses of a high-resolution lidar-derived digital elevation model from the British Columbia Open Lidar Portal (last accessed January 10, 2022 at: <https://www2.gov.bc.ca/gov/content/data/geographic-data-services/lidarbc>), shows an 11 km-long, 125°-striking, series of northeast-facing scarps across Saanich Peninsula (Fig. 1b). East of XEOLXELEK (Fig. 1c), the scarp is formed in Quaternary glacial sediments deposited during and immediately after the last glacial maximum, which occurred ~14 calibrated kiloyears before present (cal ka BP) (James et al., 2009). These glacial deposits form a 40 m-high north–south oriented, streamlined, drumlinoid ridge, parallel with southward glacial flow direction during the last glacial maximum (Fig. 1b, James et al., 2009). The scarp offsets the surface of the drumlinoid, southwest-side up, by a vertical separation of ~1.4 to 3.5 m.

Exposures of bedrock faulting and the trace of the scarp across the drumlin are consistent with a ~50° south-dipping reverse fault forming the scarp (Fig. 1b). Assuming a planar fault produced the scarp across the drumlinoid, structural contour lines of the fault plane based on the surface elevation of the scarp indicate a fault oriented 127°/50° SW. Outcrops along the fault trace east of the drumlin show planar faults formed in bedrock that dip 45°–62° south and strike between 102° and 115°. West of XEOLXELEK, we observed one bedrock fault with an orientation of 075°/36° SE, and slickenlines indicating reverse slip (Fig. 1b).

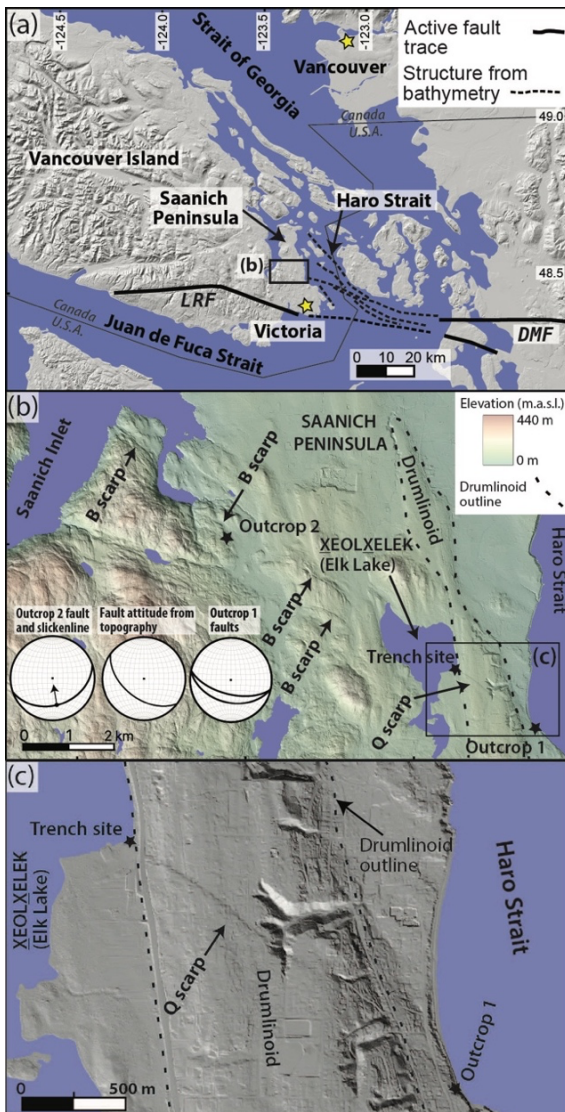


Figure 1: a) Map of southern Vancouver Island showing the Leech River fault (LRF), the Devils Mountain fault (DMF), and structures in Haro Strait. Fault traces adapted from Greene & Barrie, (2022). Basemap is from the United State Geological Survey (USGS) National Map service. b) Hillshade map coloured by elevation (meters above sea level: m.a.s.l.) of Saanich Peninsula with Quaternary (Q) and bedrock (B) scarps shown. Lower-hemisphere stereonet projections show bedrock fault plane orientations at Outcrops 1 and 2, slickenline orientation and slip sense of hanging wall at Outcrop 2, and the fault orientation derived from structural contour mapping of the Q scarp. c) Hillshade map showing the Q scarp offsetting the surface of a drumlinoid east of XEOLXELEK. Hillshade maps in (b) and (c) were derived from the BC Open Lidar digital elevation models.

PALEOSEISMIC TRENCH

On the eastern shore of XEOLXELEK (Fig. 1b), excavation of a 32 m-long paleoseismic trench and auger holes revealed deformed glacial sediments overlain by a colluvial wedge, undeformed beach sediments, and anthropogenic fill (Fig. 2). The glacial sediments, composed of diamict (Unit EB1) overlain by well-bedded silts and clay (Unit EB2), are deformed by a fault-cored monocline centered at the

scarp. The monocline results in ~ 2.3 m of vertical separation of the top of Unit EB2 assuming no erosion of this unit. This assumption is based on a consistent ~ 2 m-thickness of Unit EB2 across the monocline, and the presence of a ~ 1 m-thick, paleosol horizon (EB2b) at the top of EB2 that is continuous across the fold. Both EB1 and EB2 are offset ~ 0.2 m by gently south-dipping ($\sim 090^\circ/20^\circ$) reverse faults in the core of the monocline. South of the monocline, numerous fractures and normal faults crosscut these units and show minor offsets (<0.2 m).

A colluvial wedge (Unit EB3) we interpret as related to a single earthquake, overlies the toe of the scarp above down-thrown glacial sediments on the footwall of the fault-cored monocline (Fig. 2). This colluvial unit is a channel- or wedge-shaped body of poorly-sorted matrix-supported diamict and contains clasts of the underlying bedded clays and silts (Unit EB2). It thins both to the north, away from the scarp, and to the south, where it unconformably overlies the fold scarp. The lack of internal deformation and paleosol horizons within this unit suggest this colluvial wedge began to form after a single earthquake event and has not been subsequently deformed by a second earthquake.

A thin (<0.3 m) layer of well-sorted medium-grained sand (Unit EB4) and two units (EB5 and EB6) of anthropogenic fill, containing glass fragments and bricks, overlie the older units. We interpret these units are the result of deposition of beach sands after the deposition of the colluvial wedge, and subsequent filling with anthropogenic material during park construction adjacent to XEOLXELEK.

DISCUSSION

Our observations suggest the topographic scarp observed on Saanich Peninsula was the result of a single Holocene earthquake. During the most recent glacial maximum at 14 cal ka BP, a continental ice sheet flowed southward across the peninsula (e.g., James et al., 2009) resulting in the formation of the drumlinoid ridge east of XEOLXELEK (Fig. 1b). If the scarp deformed the surface of the drumlin before deglaciation, it would have been eroded away by the overriding glacier. In addition, the paleosol at the top of the youngest deformed unit in our paleoseismic trench (Unit EB2) indicates this unit was exposed subaerially. A drop in relative sea level, due to isostatic rebound, likely exposed the trench site subaerially between 12.2 and 12.0 cal ka BP (James et al., 2009), suggesting soil formation and subsequent deformation after this date. Although there are no historical records of a surface-rupturing earthquake on Saanich Peninsula, debris flow deposits observed in drill cores from nearby Saanich Inlet (Fig. 1) suggest several ground shaking events not corresponding to documented megathrust earthquakes on the Cascadia subduction zone (Blais-Stevens et al., 2011). The youngest of these uncorrelated deposits accumulated between 410 and 435 years BP, suggesting a youngest possible earthquake age. Further constraint of event timing using ^{14}C -dating of detrital charcoal is ongoing.

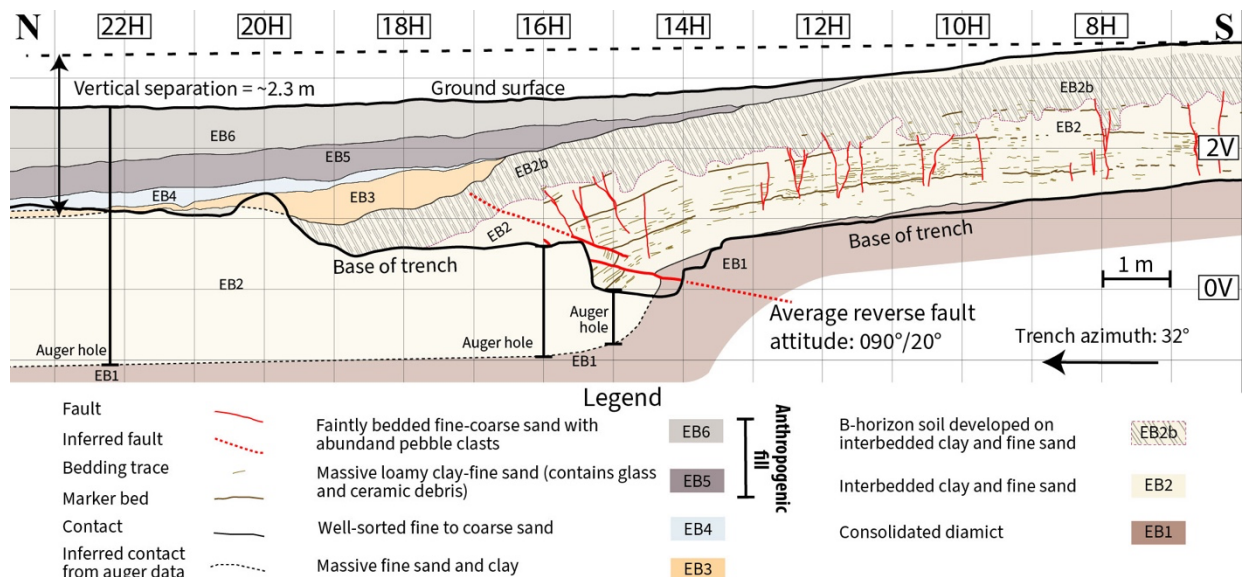


Figure 2: Interpretation of the east wall of paleoseismic trench across the XELF. Trench log from 6H to 24H, centered on the monocline and south-dipping reverse faults are shown. Contacts below trench floor were inferred using unit contacts in auger data.

The shallowly-dipping reverse faults in the paleoseismic trench ($\sim 090^\circ/20^\circ$) do not match the moderately dipping (45° to 62°) reverse faults determined from Quaternary scarps and bedrock faults, making estimation of coseismic slip and earthquake magnitude difficult. The monocline and reverse fault geometry observed in the trench resembles folds formed above a propagating reverse fault tip (e.g., Livio et al., 2020). Therefore, we hypothesize the deformation in the trench is a result of a moderately dipping fault at depth that is consistent with fault orientations beyond the trench.

To test the hypothesis of a fault-propagation fold in the paleoseismic trench and place constraints on minimum fault slip, we used FaultFold (Allmendinger, 1998; Zehnder & Allmendinger, 2000) to forward model folding above a propagating 50° -dipping reverse fault to reproduce the observed deformation (e.g., Livio et al., 2020) (Fig. 3). Fold geometry in FaultFold is based on fault geometry, the fault propagation-to-slip ratio (P/S), and the trishear angle (TS) defining the triangular area in front of the propagating fault tip that is folded (Allmendinger, 1998). As initial conditions, we assumed horizontal, undeformed glacial sediments, a 50° south-dipping fault propagating towards the center of the monocline, and a TS of 60° . We also assumed the fault would propagate from bedrock to glacial sediments at a depth of 2.7 m below the base of Unit EB2, based on preliminary geophysical (electrical resistivity) survey results. We then varied the total slip and the P/S for the basal and glacial sediments until we best reproduced the deformation observed in the trench.

We found that a 50° south-dipping reverse fault accumulating 1.83 m of slip while propagating through bedrock with a high P/S of 10 (Fig. 3a), then slipping 1.37 m while propagating through glacial sediments with a

lower P/S of 3.4 (Fig. 3b), closely reproduced the observed monocline. The P/S reduction is consistent with propagation through a less consolidated material and the P/S ratio of 3.4 is similar to P/S observed in silts and clay (Livio et al., 2020). We then initiated a minor 10° -dipping reverse fault near the tip of the main fault, and allowed it to slip 0.2 m with a P/S of 3.4 (Fig. 3c). This minor fault with a gentle dip allowed us to better match the observed fault and fold geometry in the paleoseismic trench (Fig. 3d). Although these parameters represent a non-unique solution, they show that ~ 3.2 m of total slip on a blind 50° -dipping reverse fault is consistent with the topographic analysis of the scarp and can produce a fault-propagation fold consistent with our paleoseismic trench observations.

Assuming ~ 3.2 m of coseismic slip at the surface during the surface-rupturing earthquake on the XELF, the paleo-earthquake magnitude can be roughly estimated. We neglect the slip on the minor reverse fault in the trench, because we infer that this structure nucleated near the surface (Fig. 3c), has a negligible surface area, and does not significantly contribute to moment release. Using the Wesnousky (2008) scaling relationships between average and maximum surface displacements and magnitude for reverse earthquakes, we estimate that the observed deformation was produced by a M 6.1–7.6 earthquake. However, the true uncertainty is likely greater still, as we lack constraints on surface slip along the length of the rupture trace. We also lack constraints on a potential strike-slip component of surface displacement, which would increase the net displacement and earthquake magnitude. Further analyses of the surface slip distribution, potential surface rupture length, and seismogenic depth extent could better constrain the paleo-earthquake magnitude for use in deterministic seismic hazard assessments.

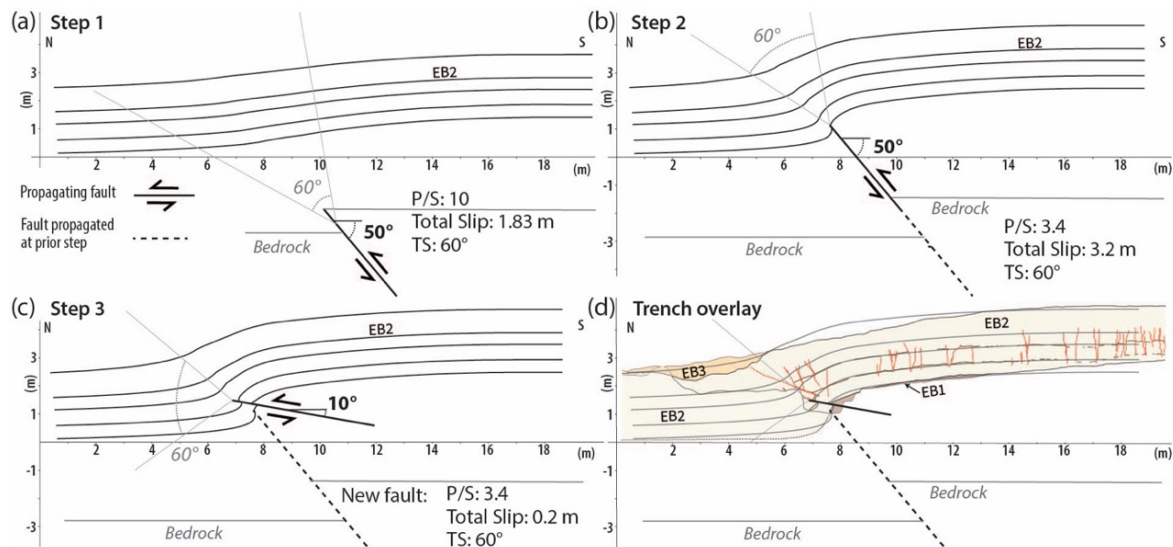


Figure 3: Forward fault-propagation fold model. a) 1.83 m of reverse fault slip and propagation through bedrock with P/S = 10. b) The fault tip has propagated to glacial sediments and P/S has dropped to 3.4. 1.37 m of fault slip (total slip of 3.2 m) is accumulated, and the fault tip has propagated close to the EB1-EB2 contact. c) A new fault dipping 10° southwest accommodates 0.2 m of slip. d) Overlay of Units EB1, EB2, and EB3 from the trench log (Fig. 2) on the final result of the model.

CONCLUSIONS

Topographic analyses and paleoseismic trenching indicate a Holocene earthquake on the newly identified XEOLXELEK–Elk Lake fault across Saanich Peninsula on southern Vancouver Island, Canada. The trench revealed evidence that a single earthquake deformed glacial sediments via a fault-propagation fold above a blind reverse fault. Fault-fold propagation modelling indicates that ~3.2 m of reverse slip on a fault propagating through two different geologic units, each with different propagation-to-slip ratios, could reproduce the observed deformation. Average surface slip of 3.2 m along a reverse fault corresponds to a M 6.1–7.6 earthquake using established fault scaling relations. Although there is substantial uncertainty associated with this estimate, an earthquake close to this magnitude would cause significant damage to the Victoria region and is worth considering in future seismic hazard assessments.

Acknowledgements: This study was conducted on the traditional territory of the WSÁNEĆ people and the authors from the University of California, Santa Barbara, University of Victoria, and Northern Arizona University acknowledge their historical relationships with the land that continue to this day. This research was supported by an NSF EAR grant # 1756943 to Dr. Morell, an NSF EAR grant # 1756834 to Dr. Regalla, funding from the USGS National Cooperative Geologic Mapping Program to Dr. Bennett, an NSERC Discovery grant # 2017-04029 and Canada Research Chair to Dr. Nissen, and an NSERC Alexander Graham Bell Canada Graduate scholarship to Finley. We thank the Capital Regional District (especially A. Mitchell, J. Mollin and M. Solomon) for access to Elk Lake Regional Park, Walter Langer for the trench excavation and associated logistics, and Simon Smith for monitoring the excavation and sharing insights into the history of XEOLXELEK. We also thank the USGS internal reviewers for their thoughtful comments on this document. Any use of trade, firm, or product names is for descriptive purposes only and does not imply endorsement by the U.S. Government

REFERENCES

- Allmendinger, R. W. 1998. Inverse and forward numerical modelling of trishear fault-propagation folds. *Tectonics*, 17 (4), 640–656.
- Blais-Stevens, A., Rogers, G. C., & Clague, J. J. 2011. A revised earthquake chronology for the last 4,000 years inferred from varve-bounded debris-flow deposits beneath an inlet near Victoria, British Columbia. *Bulletin of the Seismological Society of America*, 101 (1), 1–12.
- Greene, H.G., & Barrie, J.V., 2022. Faulting within the San Juan-southern Gulf Islands Archipelagos, upper plate deformation of the Cascadia subduction complex. *Geological Society, London, Special Publications*, 505(1), pp.SP505-2019.
- James, T. S., Gowan, E. J., Hutchinson, I., Clague, J. J., Barrie, J. V., & Conway, K. W. 2009. Sea-level change and paleogeographic reconstructions, southern Vancouver Island, British Columbia, Canada. *Quaternary Science Reviews*, 28 (13), 1200-1216
- Kukovica, J., Ghofrani, H., Molnar, S., & Assatourians, K. 2019. Probabilistic Seismic Hazard Analysis of Victoria, British Columbia: Considering an Active Fault Zone in the Nearby Leech River Valley. *Bulletin of the Seismological Society of America*, 109 (5), 2050–2062
- Livio, F., Ferrario, M., Frigerio, C., Zerboni, A., & Michetti, A. 2020. Variable fault tip propagation rates affected by near-surface lithology and implications for fault displacement hazard assessment. *Journal of Structural Geology*, 130, 103914
- Morell, K. D., Regalla, C., Amos, C., Bennett, S., Leonard, L., Graham, A., Reedy, T., Levson, V., & Telka, A. 2018. Holocene surface rupture history of an active forearc fault redefines seismic hazard in southwestern British Columbia, Canada. *Geophysical Research Letters*, 45 (210), 11–605.729
- Wesnowsky, S. G. 2008. Displacement and geometrical characteristics of earthquake surface ruptures: Issues and implications for seismic-hazard analysis and the process of earthquake rupture. *Bulletin of the Seismological Society of America*, 98(4), 1609-1632.
- Zehnder, A. T., & Allmendinger, R. W. 2000. Velocity field for the trishear model. *Journal of Structural Geology*, 22 (8), 1009-1014.